Water soluble laurate-stabilized ruthenium(0) nanoclusters catalyst for hydrogen generation from the hydrolysis of ammonia-borane: High activity and long lifetime

3 AUTHORS:

Feyyaz Durap
Dicle University
48 PUBLICATIONS **771** CITATIONS

SEE PROFILE

Mehmet Zahmakıran
Yuzuncu Yil University
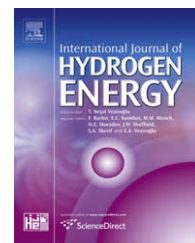**75** PUBLICATIONS **1,580** CITATIONS

SEE PROFILE

Saim Özkar
Middle East Technical University
298 PUBLICATIONS **5,245** CITATIONS

SEE PROFILE

Water soluble laurate-stabilized ruthenium(0) nanoclusters catalyst for hydrogen generation from the hydrolysis of ammonia-borane: High activity and long lifetime

Feyyaz Durap[*],[1], *Mehmet Zahmakıran, Saim Özkar*

Department of Chemistry, Middle East Technical University, 06531 Ankara, Turkey

ABSTRACT

The simplest amine-borane, considered as solid hydrogen storage material, ammonia-borane (H_3NBH_3) can release hydrogen gas upon catalytic hydrolysis under mild conditions. Herein, we report the preparation of a novel catalyst, water dispersible laurate-stabilized ruthenium(0) nanoclusters from the dimethylamine-borane reduction of ruthenium(III) chloride in sodium laurate solution at room temperature. The ruthenium nanoclusters in average size of 2.6 ± 1.2 nm were isolated from the solution and well characterized by using TEM, XPS, FTIR, and UV–visible electronic absorption spectroscopy. The water dispersible laurate-stabilized ruthenium(0) nanoclusters were found to be highly active and long-live catalyst with a TOF of 75 mol H_2/mol Ru·min and TTO value of 5900 mol H_2/mol Ru in the hydrolysis of ammonia-borane at $25.0 \pm 0.1\ ^\circ C$.

© 2009 International Association for Hydrogen Energy. Published by Elsevier Ltd. All rights reserved.

1. Introduction

There have been intensive efforts for developing safe and efficient methods for hydrogen storage, a key issue of the hydrogen economy [1–3]. Amine-boranes have recently been considered among the hydrogen storage materials because of the following advantageous properties [4]: (i) having high hydrogen content, (ii) having high stability, and (iii) being environmentally benign. The simplest amine-borane being considered as solid hydrogen storage material [5–8] is ammonia-borane (AB, H_3NBH_3) possessing a low molecular weight (30.9 g/mol) and highest hydrogen content (19.6 wt%) [4]. AB is nontoxic, stable, and environmentally benign, can be handled at room temperature and can release hydrogen gas

upon catalytic hydrolysis under mild conditions (Eq. (1)) [4]. The hydrolysis occurs at appreciable rate only in the presence of a suitable catalyst at ambient temperature [9,10].

$$H_3NBH_3(aq) + 2H_2O(l) \xrightarrow{\text{catalyst}} NH_4^+(aq) + BO_2^-(aq) + 3H_2(g) \quad (1)$$

So far, the catalysts tested in the hydrolysis of ammonia-borane are platinum supported on carbon (20 wt%) [10], colloidal rhodium(0) [11], $Ni_{1-x}Pt_x$ hollow spheres [12], ruthenium(0), rhodium(0) and platinum(0) particles supported on γ-Al_2O_3 [13], various transition metal salts $RuCl_3$, $PdCl_2$, $CoCl_2$, and palladium supported carbon (Pd/C) [14], Fe(0) nanoparticles [15], Co(0)/Co_2B, Ni(0)/Ni_3B, Cu(0) nanoparticles [16], poly(N-vinyl-2-pyrrolidone) (PVP) stabilized nickel catalyst [17], hollow Ni–SiO_2 nanosphere [18] and

Pt- and Ni-based alloy catalysts [19]. The use of colloidal or supported particles as active catalyst in the hydrolysis of ammonia-borane implies that reducing the particle size can cause an increase in the catalytic activity as the fraction of surface atoms increases with the decreasing particle size [20]. Accordingly, the transition metal nanoclusters can be employed as catalyst for this reaction as well. For this purpose, the transition metal nanoclusters need to be stabilized to certain extend [21]. In the preparation of water-soluble transition metal nanoclusters, electrostatic stabilization by anions [22,23] is necessary to prevent their agglomeration into the bulk metal. Here we report, for the first time, the preparation and characterization of water dispersible ruthenium(0) nanoclusters stabilized by laurate (dodecanoate) anion and their employment as catalyst in the hydrolysis of ammonia-borane.

2. Experimental

Ruthenium(III) chloride trihydrate ($RuCl_3 \cdot 3H_2O$, 99.5%, Sigma), sodium laurate ($C_{12}H_{23}NaO_2$, 99%, Fluka), dimethylamine-borane (DMAB) ((CH_3)$_2NHBH_3$, 97%, Sigma), and ammonia-borane (AB, H_3NBH_3, 99%, Sigma) were purchased from Aldrich. Ethanol was purchased from Merck. Deionized water was distilled by water purification system (Milli Q-pure WS). All glassware and Teflon coated magnetic stir bars were cleaned with acetone, followed by copious rinsing with distilled water before drying in an oven at 150 °C.

2.1. The preparation of laurate-stabilized ruthenium(0) nanoclusters

Ruthenium(III) chloride trihydrate of 4.2 mg ($RuCl_3 \cdot 3H_2O$, 0.02 mmol) was dissolved in 10 mL deionized water and 44.5 mg sodium laurate ($C_{12}H_{23}NaO_2$, 0.2 mmol) was added into this solution and stirred half an hour at room temperature. Then 59 mg dimethylamine-borane ((CH_3)$_2NHBH_3$, 1.0 mmol) was added into this mixture, after 4 h the color of solution completely changed into deep brown at room temperature. The laurate-stabilized ruthenium(0) nanoclusters, dark brown in color, were found to be stable in aqueous media (no precipitation was observed after a month of storage) under ambient conditions.

2.2. The separation of laurate-stabilized ruthenium(0) nanoclusters as a solid material

The laurate-stabilized ruthenium(0) nanoclusters were separated from the solution by precipitation with ethanol (20 mL) followed by centrifugation (5000 rpm, for 1 h). The laurate-stabilized ruthenium(0) nanoclusters were separated as a solid material washed with 30% (v/v) water/ethanol mixture to remove water soluble impurities.

2.3. Transmission electron microscopy (TEM) analyses

One drop of the laurate-stabilized ruthenium(0) nanoclusters solution was deposited on the chloroform cleaned, carbon coated Cu TEM grid and the solvent was then evaporated and analyzed by using Philips CM-12 TEM with a 70 μm lens operating at 100 kV and with a 2.0 Å point-to-point resolution. Samples were examined at magnification between 100 and 400K. Particle size analysis was performed using the public domain NIH Image J 1.62 program developed at the U.S. National Institutes of Health and available on the Internet at http://rsb.info.nih.gov/nih-image/. For each particle, the diameter was calculated from the area by assuming that the nanoclusters are spherical. Size distributions are quoted as the mean diameter ± the standard deviation.

2.4. X-ray photoelectron spectroscopy (XPS) analyses

The XPS analysis was performed on a Physical Electronics 5800 spectrometer equipped with a hemispherical analyzer and using monochromatic Al Kα radiation (1486.6 eV, the X-ray tube working at 15 kV, 350 W and pass energy of 23.5 keV). The peak fitting of original spectrum has been done by mixing (50:50%) of both Lorentzian and Gaussian functions on Origin 7.0 program.

2.5. Fourier transform infrared spectroscopy (FTIR) analyses

The sample prepared for the XPS analysis was also used for the FTIR analysis. FTIR spectrum of both sodium laurate and the laurate-stabilized ruthenium(0) nanoclusters was taken from KBr pellet on a Nicolet 510 FTIR Spectrophotometer using Omnic software.

2.6. ^{11}B NMR analyses

^{11}B NMR spectra were recorded on a Bruker Avance DPX 400 with an operating frequency of 128.15 MHz for ^{11}B. D_2O and $BF_3 \cdot (C_2H_5)_2O$ were used as a lock and an external reference, respectively. At the end of the hydrolysis reaction, the resulting solutions were filtered and the filtrates were collected for ^{11}B NMR analysis.

2.7. Method for testing the catalytic activity of laurate-stabilized ruthenium(0) nanoclusters in the hydrolysis of H_3NBH_3

The catalytic activity of laurate-stabilized ruthenium(0) nanoclusters in the hydrolysis of ammonia-borane was determined by measuring the rate of hydrogen generation. To determine the rate of hydrogen generation the catalytic hydrolysis of ammonia-borane was performed using a Fischer–Porter pressure bottle modified with Swagelock TFE-sealed quick connects and connected to an Omega PX-302 pressure transducer interfaced through an Omega D1131 digital transmitter to a computer using the RS-232 module. The progress of an individual hydrolysis reaction was followed by monitoring the increase of H_2 pressure on Lab View 8.0 program. The pressure versus time data was processed using Microsoft Office Excel 2003 and Origin 7.0 then converted into the proper unit [volume of hydrogen (mL)]. In a typical experiment, 30.9 mg (1 mmol) H_3NBH_3 was dissolved in 10 mL water, (corresponding to a maximum amount of 3 mmol = 67 mL H_2 at 25.0 ± 0.1 °C). This

solution was transferred with a 50 mL glass-pipette into the FP bottle thermostated at $25.0 \pm 0.1\,°C$. Then, aliquots of laurate-stabilized ruthenium(0) nanoclusters from the stock solution (2 mM) was transferred into the FP bottle. The experiment was started by closing the FP bottle connected to the pressure transducer and turning on the stirring at 1000 rpm simultaneously. In addition to the volumetric measurement of the hydrogen evolution, the conversion of ammonia-borane to ammonium metaborate was also checked by comparing the intensities of signals of ammonia-borane and metaborate anion at $\delta = -23.9$ and 9 ppm, respectively, in the ^{11}B NMR spectra of the solution [24].

2.8. Determination of activation energy for the laurate-stabilized ruthenium(0) nanoclusters catalyzed hydrolysis of ammonia-borane

In a typical experiment, the hydrolysis of 10 mL of 200 mM H_3NBH_3 catalyzed by 1 mM laurate-stabilized ruthenium(0) nanoclusters was performed by following the same way described in Section 2.7 at various temperatures (5, 10, 15, 20, 25, 30, 35 °C) in order to obtain the activation energy (E_a). In order to find the activation energy for the RuCl$_3$ catalyzed hydrolysis of ammonia-borane, the hydrolysis of 10 mL of 200 mM H_3NBH_3 catalyzed by 1 mM ruthenium(III) chloride was performed at various temperatures (10, 20, 30, 40 and 50 °C).

2.9. Determination of the catalytic lifetime of laurate-stabilized ruthenium(0) nanoclusters in the hydrolysis of ammonia-borane

The catalytic lifetime of laurate-stabilized ruthenium(0) nanoclusters in the hydrolysis of ammonia-borane was determined by measuring the total turnover number (TTO). Such a lifetime experiment was started with a 10 mL solution containing 1.0 mM laurate-stabilized ruthenium(0) nanoclusters and 600 mM H_3NBH_3 at $25.0 \pm 0.1\,°C$. When the complete conversion is achieved, more ammonia-borane was added and the reaction was continued in this way until no hydrogen gas evolution was observed. Under the same conditions, the catalytic lifetime of ruthenium(III) chloride (0.9 mg, 0.0035 mmol Ru) in the hydrolysis of ammonia-borane was determined by measuring the total turnover number.

2.10. Determination of the recyclability of laurate-stabilized ruthenium(0) nanoclusters in the hydrolysis of ammonia-borane

The recyclability of laurate-stabilized ruthenium(0) nanoclusters in the hydrolysis of ammonia-borane was determined by a series of experiments started with a 10 mL solution containing 1.0 mM laurate-stabilized ruthenium(0) nanoclusters and 100 mM H_3NBH_3 at $25.0 \pm 0.1\,°C$. When the complete conversion is achieved, immediately, another equivalent of H_3NBH_3 (100 mM) was added to leading further hydrogen evolution from the reaction mixture.

3. Results and discussion

3.1. Preparation and characterization of water dispersible laurate-stabilized ruthenium(0) nanoclusters

The water dispersible laurate-stabilized ruthenium(0) nanoclusters were prepared from the reduction of ruthenium(III) chloride solution by dimethylamine-borane $((CH_3)_2HNBH_3$, DMAB) in the presence of sodium laurate at room temperature. Without adding sodium laurate in aqueous solution, the ruthenium(0) nanoclusters formed by DMAB reduction of RuCl$_3$ readily agglomerate ultimately to the bulk metal precipitating out of the solution. In the presence of sodium laurate, however, the ruthenium(0) nanoclusters are highly stable, no formation of bulk metal is observed in solution even after one month of storage, demonstrating the role of laurate anion in the stabilization of ruthenium(0) nanoclusters. It should be noted that the laurate concentration should be 10 times more than that of ruthenium for the preparation of stable ruthenium(0) nanoclusters, as we observed the formation of bulk ruthenium(0) metal under the conditions, in which [Laurate]/[Ru] < 10. Laurate-stabilized ruthenium(0) nanoparticles were characterized by using TEM, XPS, FTIR, and UV–vis spectroscopic methods. The formation of laurate-stabilized ruthenium(0) nanoclusters could be followed by monitoring the UV–vis electronic absorption spectra as shown in Fig. 1. The starting solution of ruthenium(III) chloride shows an absorption band at 410 nm, which disappears when all of the Ru^{3+} are completely reduced to ruthenium(0) [25].

Fig. 2a and b shows the transmission electron microscopy (TEM) images of the sample harvested from the reaction solution when the reduction of ruthenium(III) to ruthenium(0) is completed. The histogram in Fig. 2c was constructed from the TEM image by using NIH image program [26], whereby 347 non-touching particles were counted. The mean particle size of the laurate-stabilized ruthenium(0) nanoclusters was found to be 2.6 ± 1.2 nm.

The laurate-stabilized ruthenium(0) nanoclusters could be isolated from the reaction solution by precipitation with
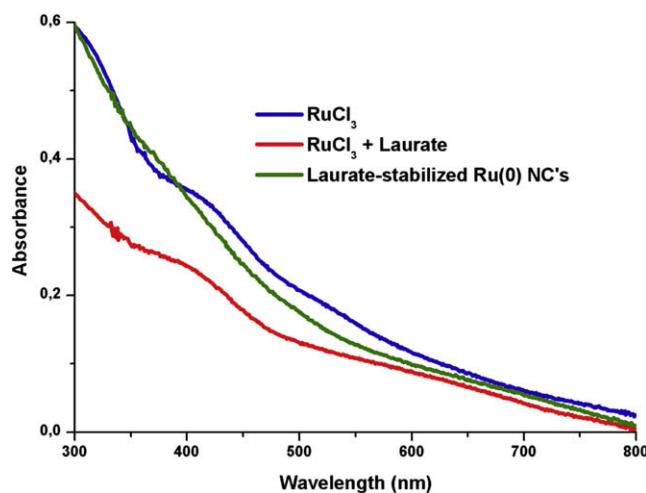

Fig. 1 – UV–vis absorption spectra of RuCl$_3$ solution, RuCl$_3$ in sodium laurate solution and laurate-stabilized ruthenium(0) nanoclusters' solution.
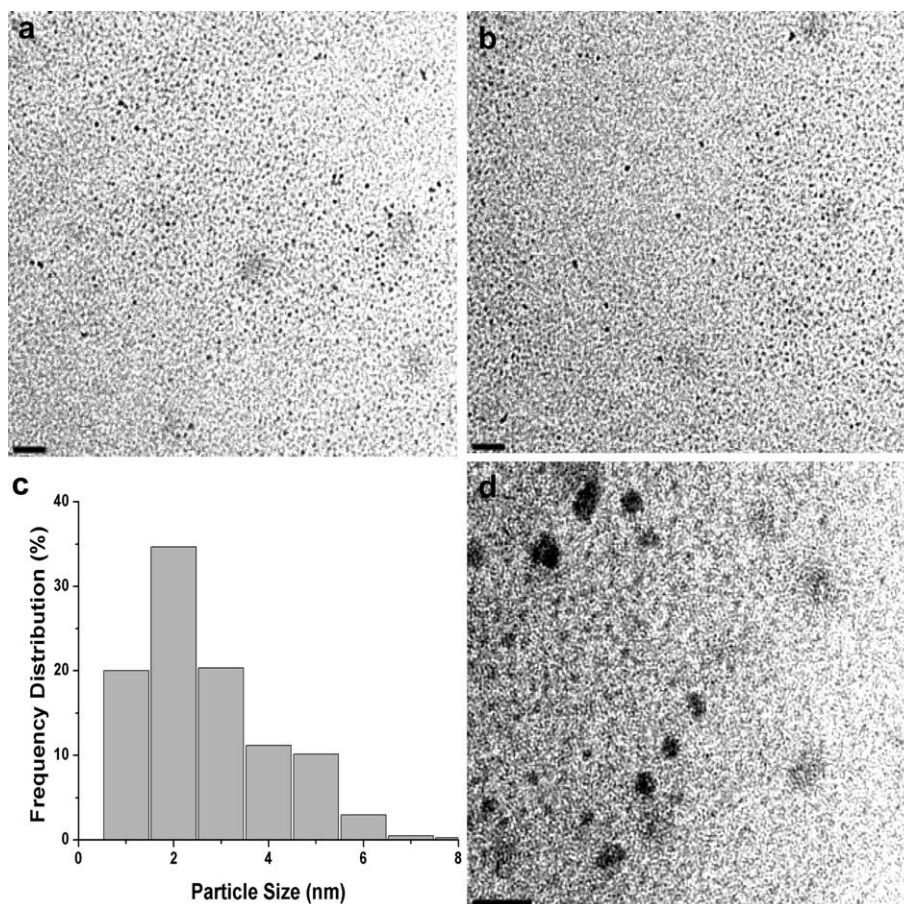
Fig. 2 – (a) and (b) are TEM images of laurate-stabilized ruthenium(0) nanoclusters taken from different regions on copper grid, (c) associated histogram constructed from TEM images given (a) and (b), (d) TEM image of laurate-stabilized ruthenium(0) nanoclusters at the end of fifth run in the hydrolysis of ammonia-borane (all scale bars represent 50 nm).

ethanol followed by centrifugation at 5000 rpm for 1 h and washing with water/ethanol mixture to remove water soluble impurities. The isolated sample of laurate-stabilized ruthenium(0) nanoclusters was used for the XPS analysis of the nanocluster surface composition. The main peaks observed in the survey scan XPS (Fig. 3a) are C 1s, Ru 3d, Ru 3p and O 1s at 285, 280–285, 460–480 and 530 eV, respectively. Unfortunately, the overlap of the C 1s and Ru $3d_{3/2}$ peaks around 285 eV makes it difficult to analyze this range for ruthenium correctly. Therefore, only Ru $3p_{3/2}$ peak had to be used for the ruthenium analysis (Fig. 3b). The Ru $3p_{3/2}$ feature fits well to two deconvoluted peaks at 461.4 and 463.5 eV, readily assigned to the Ru(0) $3p_{3/2}$ [27,28], and Ru(IV) $3p_{3/2}$ [27], respectively. Formation of ruthenium(IV) oxide on the surface of ruthenium(0) particles is a well known phenomenon [28] and most likely occurs during the XPS sampling.

The existence of laurate anions in the isolated nanoclusters sample was examined by FTIR spectroscopy. Comparison of the FTIR spectra of both the laurate-stabilized ruthenium(0) nanoclusters sample and the sodium laurate taken from KBr pellet in the frequency range of 1250–2200 and 2400–3750 cm^{-1} (Fig. 4) shows that the absorption bands due to the C–H stretching remain essentially unaltered while the bands due to the C–O stretching of laurate anion undergo

a shift to the lower frequency upon adsorption on the surface of ruthenium(0) nanocluster [29] (Fig. 4). These results indicate unequivocally the existence of laurate anions in the ruthenium(0) nanoclusters sample and most likely adsorbed on the nanoclusters surface.

3.2. Testing the catalytic activity of water dispersible laurate-stabilized ruthenium(0) nanoclusters in the hydrolysis of ammonia-borane and the effect of laurate concentration on the catalytic activity of ruthenium(0) nanoclusters

Prior to starting further kinetic experiments for the laurate-stabilized ruthenium(0) nanoclusters catalyzed hydrolysis of ammonia-borane, we investigated the effect of [Laurate]/[Ru] ratio on the catalytic activity of ruthenium(0) nanoclusters in the hydrolysis of ammonia-borane. The effect of the stabilizer concentration on the catalytic activity of the ruthenium(0) nanoclusters ([Ru] = 0.25 mM), which had been prepared at various [Laurate]/[Ru] ratios (10, 20, 30, 40), was investigated by performing the catalytic hydrolysis of 100 mM ammonia-borane at 25.0 ± 0.1 °C. The rates of hydrogen generation were found to be 5.5, 4.2, 3.4, 1.9 mL H$_2$/min for [Laurate]/[Ru] ratios of 10, 20, 30 and 40, respectively. The highest catalytic activity
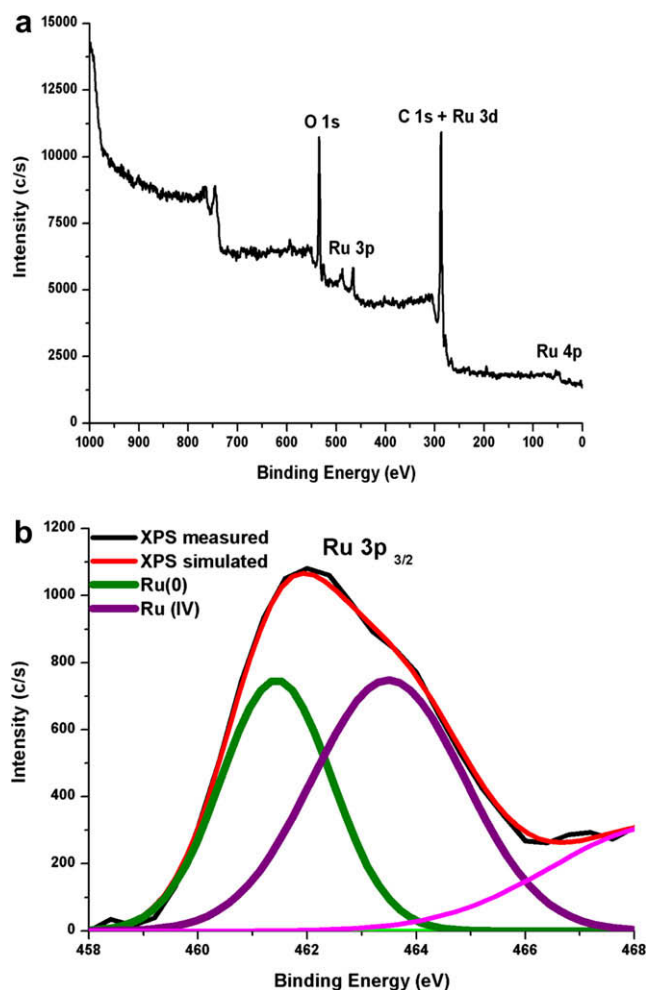
Fig. 3 – (a) X-ray photoelectron spectrum of laurate-stabilized ruthenium(0) nanoclusters and (b) Ru 3p$_{3/2}$ signal in the region of 450–469 eV and simulated peak fitting.

Fig. 4 – FTIR spectra of sodium laurate and laurate-stabilized ruthenium(0) nanoclusters taken from KBr pellets.

was achieved for ruthenium(0) nanoclusters stabilized by [Laurate]/[Ru] ratio of 10. It is worth to note that the laurate ion is adsorbed on the nanoclusters surface generating a double layer, which provides electrostatic stabilization against agglomeration of the particles. The laurate ion adsorbed on the nanoclusters surface is in dynamic equilibrium with the laurate ion in the solution, so that some of the surface metal atoms are still available providing active sites for the catalysis. However, at higher stabilizer concentration, the surface active sites are blocked by the laurate ions adsorbed on the surface and the catalytic activity decreases with the increasing concentration of the laurate ion. The [Laurate]/[Ru] ratio around 10 appears to be the optimum one so it was concluded to start the further kinetic experiments with the [Laurate]/[Ru] ratio of 10 for ruthenium(0) nanoclusters.

The laurate-stabilized ruthenium(0) nanoclusters were found to be highly active catalyst for the hydrolysis of ammonia-borane. Fig. 5a shows the plots of the volume of hydrogen generated versus time during the catalytic hydrolysis of 100 mM ammonia-borane solution in the presence of laurate-stabilized ruthenium(0) nanoclusters in different ruthenium concentrations at $25.0 \pm 0.1\,^{\circ}$C.
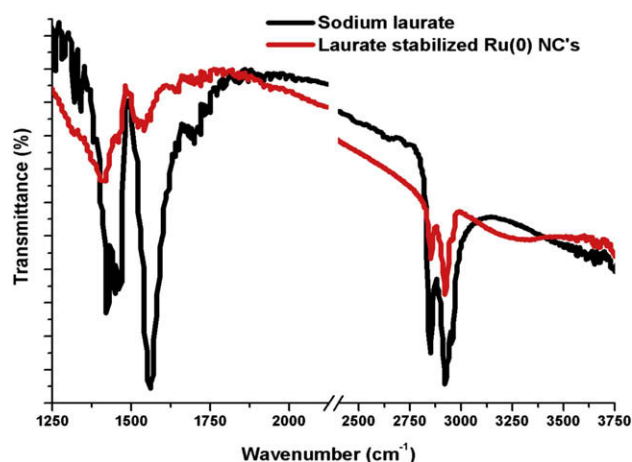
The linear hydrogen generation starts without induction period and continues until the complete hydrolysis of ammonia-borane. For example, using ruthenium(0) nanoclusters in 0.25 mM concentration leads to a complete hydrogen release (3.0 mol H_2/mol H_3NBH_3) within 22 min at $25.0 \pm 0.1\,^{\circ}$C [30]. The quantity of ammonia liberated during the hydrolysis of ammonia-borane has been found to be negligible when the catalyst concentration is less than 0.06 mol% and the substrate concentration is lower than 6 wt% [14]. Expectedly the control tests using copper(II) sulfate trap with acid/base indicators showed no ammonia evolution in detectable amount in the experiments performed in this study. Fig. 5b shows the plots of volume of hydrogen generated versus time in the hydrolysis of 200 mM H_3NBH_3 catalyzed by laurate-stabilized ruthenium(0) nanoclusters ([Ru] = 1.0 mM) at various temperatures. While hydrogen evolution starts immediately at high temperature as expected because a preformed catalyst is used, a short induction period of less than 2 min is observable at $5\,^{\circ}$C. This might be attributed to the slow activation of the catalyst at low temperature. It is worth to note that using laurate-stabilized ruthenium(0) nanoclusters in 1.0 mM Ru concentration (substrate/catalyst ratio = 200) leads to a complete H_2 release (3.0 mol H_2/mol AB) within 8 min corresponding to a TOF value of 75 mol H_2/mol Ru·min in air at $25.0 \pm 0.1\,^{\circ}$C. This is a remarkable TOF value since apart of Manners' colloidal Rh(0) which, however, has very low recyclability and lifetime [11], the highest TOF known for the catalytic ammonia-borane hydrolysis is 74 mol H_2/mol Pt·min [31], obtained by Pt/Al$_2$O$_3$ under Ar atmosphere at $25\,^{\circ}$C. Furthermore, the laurate-stabilized ruthenium(0) nanoclusters show significant catalytic activity even at low temperatures (TOF = 16 mol H_2/mol Ru·min at $5 \pm 0.1\,^{\circ}$C). The rate constants of hydrogen generation from the hydrolysis of ammonia-borane were measured from the linear portions of the plots given in Fig. 5b at seven different temperatures in the range of 5–35 $^{\circ}$C and used for the calculation of activation energy ($E_a = 47.0 \pm 2.2$ kJ/mol) from the Arrhenius plot (Fig. 6).

This value is higher than the activation energy value obtained in hydrolysis of ammonia-borane catalyzed by Ru(0)

Fig. 6 – Arrhenius plot for the laurate-stabilized ruthenium(0) nanoclusters catalyzed hydrolysis of ammonia-borane, $[H_3NBH_3] = 200$ mM and $[Ru] = 1.0$ mM.
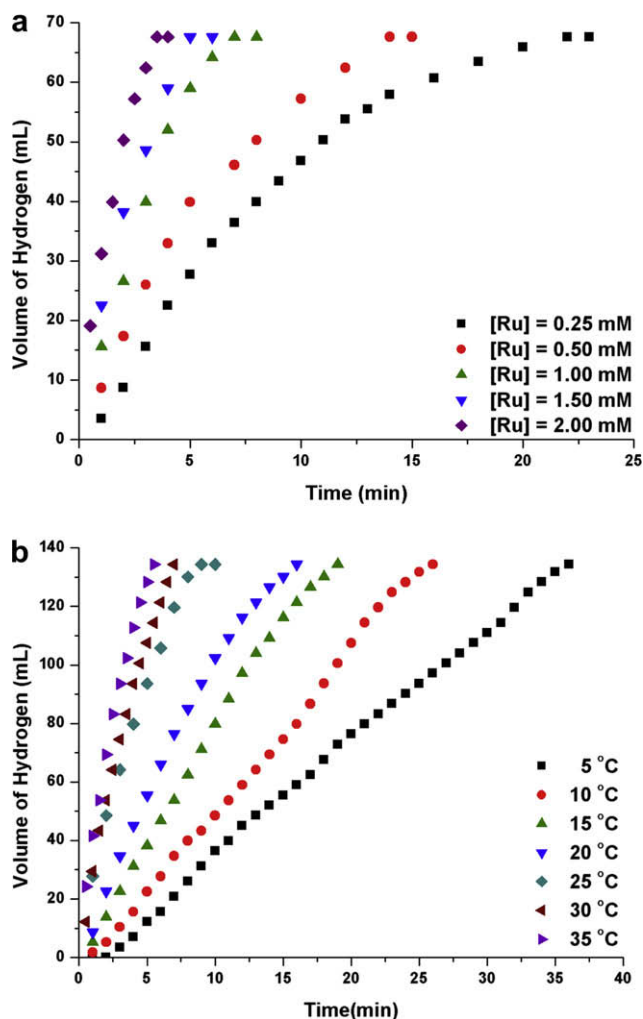
Fig. 5 – (a) The volume of hydrogen versus time graph for the laurate-stabilized ruthenium(0) nanoclusters catalyzed hydrolysis of ammonia-borane for different Ru concentrations at 25.0 ± 0.1 °C, (b) The volume of hydrogen versus time graph for the laurate-stabilized ruthenium(0) nanoclusters catalyzed hydrolysis of ammonia-borane at different temperatures, $[Ru] = 1.0$ mM, $[AB] = 200$ mM.

The decrease in catalytic activity in subsequent runs may be attributed to both the passivation of nanoclusters surface by increasing boron products, e.g. metaborate, which decreases accessibility of active sites [11], and the aggregation of ruthenium(0) nanoclusters as seen from the TEM image (Fig. 2d) of the sample harvested after the fifth run of hydrolysis. Nevertheless, the laurate-stabilized ruthenium(0) nanoclusters show a reasonable catalytic lifetime (5900 turnovers) over 3 h before deactivation in the AB hydrolysis at 25.0 ± 0.1 °C (Fig. 8). Moreover, it should be noted that the laurate-stabilized ruthenium(0) nanoclusters provide approximately 3-fold higher TTO than the bulk ruthenium(0) metal formed in situ during the $RuCl_3$ by

nanoclusters supported on γ-Al_2O_3 ($E_a = 23$ kJ/mol) in which the ruthenium(0) nanoclusters are partially free, since they interact only on one side with the external surface of support. However, the laurate-stabilized ruthenium(0) nanoclusters still provide lower activation energy than $RuCl_3$ ($E_a = 66.1 \pm 3.3$ kJ/mol) and the other catalysts reported in the literature for the same reaction using different catalysts: 70 kJ/mol for Ni powder [12], 57 kJ/mol for $Ni_{0.97}Pt_{0.03}$ hollow spheres [12], and 62 kJ/mol for Co/γ-Al_2O_3 [24]. The recyclability and catalytic lifetime of the laurate-stabilized ruthenium(0) nanoclusters were also explored. Immediately following a hydrolysis reaction, a second batch of AB was added to the reactor leading further hydrogen evolution from the reaction mixture. Fig. 7 shows the results of recyclability tests for the laurate-stabilized ruthenium(0) nanoclusters up to fifth run. The laurate-stabilized ruthenium(0) nanoclusters retain 53% of their initial catalytic activity in the hydrolysis of ammonia-borane in the fifth run.
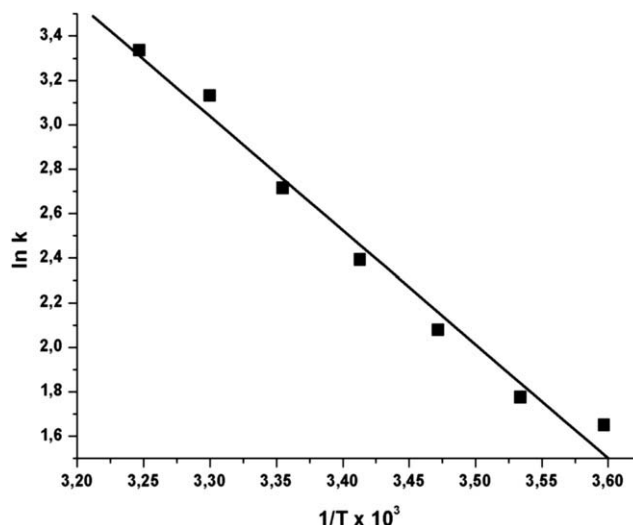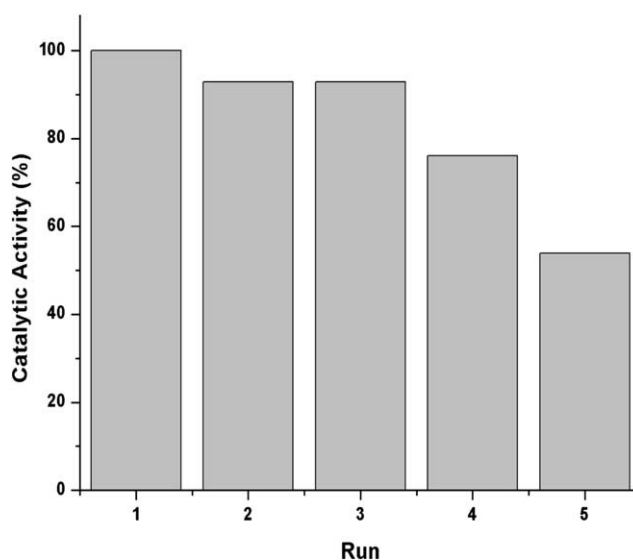

Fig. 7 – Catalytic activity of the laurate-stabilized ruthenium(0) nanoclusters as the percentage of their initial catalytic activity in the successive catalytic runs for the hydrolysis of ammonia-borane 25.0 ± 0.1 °C.
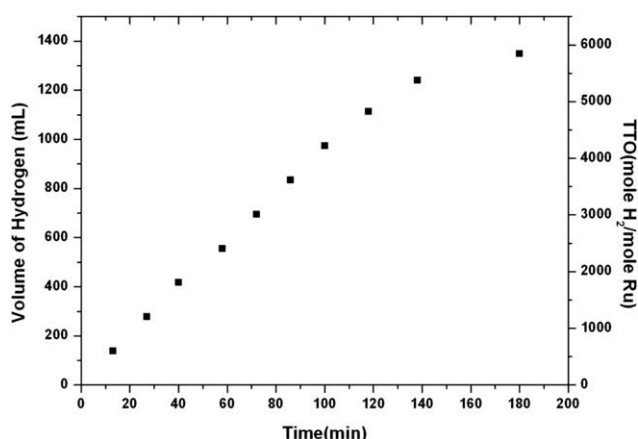
Fig. 8 – The total turnover number (TTO) and volume of hydrogen (mL) versus time plot for the laurate-stabilized ruthenium(0) nanoclusters catalyzed hydrolysis of ammonia-borane starting with 1.0 mM Ru in 10 mL at $25.0 \pm 0.1\,°C$.

which TTO value of 2000 was observed under the same conditions in the hydrolysis of ammonia-borane.

4. Conclusion

In summary, we have demonstrated that the water soluble ruthenium(0) nanoclusters $(2.6 \pm 1.2\,nm)$ can easily be prepared by the dimethylamine-borane reduction of $RuCl_3$ in sodium laurate solution at room temperature. The water dispersible laurate-stabilized ruthenium(0) nanoclusters exhibit high catalytic activity (75 mol H_2/mol Ru·min) and long catalytic lifetime (5900 mol H_2/mol Ru) in the hydrolysis of ammonia-borane in air at $25.0 \pm 0.1\,°C$.

Acknowledgements

REFERENCES

[1] Basic research needs for the hydrogen economy, report of the basic energy sciences workshop on hydrogen production, storage and use, May 13–15, 2003, Office of Science, U.S. Department of Energy, <www.sc.doe.gov/bes/hydrogen.pdf>.

[2] Turner J, Sverdrup G, Mann K, Maness PG, Kroposki B, Ghirardi M, et al. Renewable hydrogen production. Int J Energy Res 2008;32:379–407.

[3] Berg AWCV, Arean CO. Materials for hydrogen storage: current research trends. Chem Commun 2008:668–81.

[4] Basic research needs catalysis for energy, report from the US Department of Energy, basic energy sciences workshop report, August 6–8, 2007. <http://www.sc.doe.gov/bes/reports/list.html>.

[5] Marder T. Will we soon be fueling our automobiles with ammonia-borane? Angew Chem Int Ed 2007;46:8116–8.

[6] Stephens FH, Pons V, Baker TR. Ammonia-borane: the hydrogen source par excellence? Dalton Trans 2007:2613–26.

[7] Xu Q, Chandra M. A portable hydrogen generation system: catalytic hydrolysis of ammonia-borane. J Alloys Compd 2007;446–447:729–32.

[8] Umegaki T, Yun J-M, Zhang X-B, Shioyama H, Kuriyama N, Xu Q. Boron- and nitrogen-based chemical hydrogen storage materials. Int J Hydrogen Energy 2009;34:2303–11.

[9] Chandra M, Xu Q. Catalytic activities of non-noble metals for hydrogen generation from aqueous ammonia-borane at room temperature. J Power Sources 2006;163:364–70.

[10] Chandra M, Xu Q. A high performance hydrogen generation system: transition metal-catalyzed dissociation and hydrolysis of ammonia-borane. J Power Sources 2006;156:190–4.

[11] Clark TJ, Whittell GR, Manners I. Highly efficient colloidal cobalt- and rhodium-catalyzed hydrolysis of H_3NBH_3 in air. Inorg Chem 2007;46:7522–7.

[12] Cheng F, Ma H, Li Y, Chen J. $Ni_{1-x}Pt_x$ ($x = 0$–0.12) hollow spheres as catalysts for hydrogen generation from ammonia-borane. Inorg Chem 2007;46:788–94.

[13] Chandra M, Xu Q. Room temperature hydrogen generation from aqueous ammonia-borane using noble metal nano-clusters as highly active catalysts. J Power Sources 2007;168:135–42.

[14] Ramachandran PV, Gagare PD. Preparation of ammonia-borane in high yield and purity, methanolysis, and regeneration. Inorg Chem 2007;46:7810–7.

[15] Yan JM, Zang XB, Han S, Shioyama H, Xu Q. Iron-nanoparticle catalyzed hydrolytic dehydrogenation of ammonia-borane for chemical hydrogen storage. Angew Chem Int Ed 2008;47:2287–9.

[16] Kalindindi SB, Indirani M, Jagirdar BR. First row transition metal ion-asisted ammonia-borane hydrolysis for hydrogen generation. Inorg Chem 2008;47:7424–9.

[17] Umegaki T, Yan J-M, Zhang X-B, Shioyama H, Kuriyama N, Xu Q. Preparation and catalysis of poly(N-vinyl-2-pyrrolidone) (PVP) stabilized nickel catalyst for hydrolytic dehydrogenaration of ammonia borane. Int J Hydrogen Energy 2009;34:3816–22.

[18] Umegaki T, Yan J-M, Zhang X-B, Shioyama H, Kuriyama N, Xu Q. Hollow Ni–SiO_2 nanosphere-catalyzed hydrolytic dehydrogenation of ammonia borane for chemical hydrogen storage. J Power Sources 2009;191:209–16.

[19] Yao CF, Zhuang L, Cao YL, Ai XP, Yang HX. Hydrogen release from hydrolysis of borazane on Pt- and Ni-based alloy catalysts. Int J Hydrogen Energy 2008;33:2462–7.

[20] Pool R. Clusters: strange morsels of matter: when metals or semiconductor are shrunk down to clumps only 10 or 100 atoms in size, they become a ''totally new class of materials'' with potentially valuable applications. Science 1990;248:1186–8.

[21] Özkar S, Finke RG. Nanocluster formation and stabilization fundamental studies. 2. Proton sponge as an effective H^+ scavenger and expansion of the anion stabilization ability series. Langmuir 2002;18:7653–62.

[22] Aiken JD, Finke RG. A review of modern transition-metal nanoclusters: their synthesis, characterization, and applications in catalysis. J Mol Catal A Chem 1999;145:1–44.

[23] Yang J, Deivaraj TC, Too HP, Lee YJ. Acetate stabilization of metal nanoparticles and its role in the preparation of metal nanoparticles in ethylene glycol. Langmuir 2004;20:4241–5.

[24] Chandra M, Xu Q. Dissociation and hydrolysis of ammonia-borane with solid acids and carbon dioxide: an efficient hydrogen generation system. J Power Sources 2006;159:855–60.

[25] Miyazaki A, Balint I, Aika K, Nakano Y. Preparation of ruthenium nanoparticles supported on γ-Al_2O_3 and its novel catalytic activity for ammonia synthesis. J Catal 2001;204:364–71.

[26] Hutchison JE, Woehrle GH, Özkar S, Finke RG. Analysis of nanoparticle transmission microscopy data using a public-domain image-processing program, image. Turkish J Chem 2006;30:1–13.

[27] Wagner C, Riggs WM, Davis LE, Moulder JF, Muilenberg GE, editors. Handbook of X-ray photoelectron spectroscopy, vol. 55. Physical Electronic Division, Minnesota: Perkin–Elmer; 1979. p. 344.

[28] Park KW, Choi JH, Kwon BK, Lee SA, Sung YE, Ha HY, et al. Chemical and electronic effects of Ni in Pt/Ni and Pt/Ru/Ni alloy nanoparticles in methanol electrooxidation. J Phys Chem B 2002;106:1869–77.

[29] Xu SW, Zheng JP, Tong L, Yao KD. Interaction of functional groups of gelatin and montmorillonite in nanocomposite. J App Polym Sci 2006;101:1556–61.

[30] In addition to the volumetric measurement of the hydrogen evolution, the conversion of ammonia-borane to ammonium metaborate was also checked by comparing the intensities of signals of ammonia-borane and metaborate anion at $\delta = -23.9$ and 9 ppm, respectively, in the ^{11}B NMR spectra of the solution (see Refs. [11,12]).

[31] The TOF value has not been reported for Pt/γ-Al_2O_3 catalyzed hydrolysis of AB in the respective article (see Ref. [12]) but can be estimated from the data given: metal/AB = 0.018 and complete hydrogen release within 0.75 min.